Near-bed flow over a fixed gravel bed

H. Friedrich
University of Auckland, New Zealand

S.M. Spiller & N. Rüther
Department of Hydraulic and Environmental Engineering, NTNU – Norwegian University of Science and Technology, Trondheim, Norway

ABSTRACT: Advances in measurement technologies allow more detailed studies of near-bed flow fields over rough surfaces. Flow measurements over a gravel-bed mold are undertaken at the Fluid Mechanics Laboratory of the University of Auckland. The flume in use is 0.45-m wide and 19-m long. Nortek's Vectrino II profiler is used to measure the flow. Flow data are obtained over a region of interest of 0.150-m length and 0.102-m width, over which 425 samples are obtained. Upstream and downstream of the region of interest, the fixed gravel bed is extended, to reduce any disturbance of the approaching uniform flow. The flow measurements cover both, the interfacial region between gravel-bed elevation troughs and crests, as well as the region beyond the roughness elements. The individual time series' are post-processed and average flow velocity components are obtained. To showcase the potential of the applied procedure, vertical slices and a horizontal layer of near-bed flow fields are presented. It is shown that near-bed flow fields strongly interact with the gravel bed, as we already now. The advancement is in the detailed 3D representation of the near-bed flow fields, allowing any of the 14450 uniformly distributed flow data nodes to be analysed in the 3D domain. Data affected by roughness tops protruding into the sample volume can be identified with the obtained DEM. Further work is needed to compare presented data with high-resolution flow fields obtained with more widely tested instrumentation, to quantify the near-bed flow, as well as to the examine turbulent flow properties in more detail, to better understand the processes that take place at the gravel-bed boundary.

1 INTRODUCTION

The study of near-bed flows over mobile sediment beds is challenging. On the one hand there exists the measurement challenge, needing equipment that is suitable to provide near-bed flow data, which can be spatially and temporally decomposed. On the other hand, the mobile nature of the boundary does not allow assigning detailed measurement values to a known spatial boundary. Especially the flow fields in the area between the grain tops and grain troughs, the interfacial layer, are poorly understood, due to the challenge of obtaining reliable data. Several recent studies provided new insights into near-bed flow fields. In general, gravel-bed environments belong to the hydraulically rough regime, with an insignificant viscous sublayer thickness (Smart 1999). Nikora et al. (2001) revolutionised our research with the presentation of double-averaged momentum equations, which since then have been used in various other studies. Aberle et al. (2008) applied the double-averaging methodology to study the spatial heterogeneity of near-bed flows. They found that for an identical bed, discharge did not control the form-induced stress distribution. It must be pointed out that the gravel-bed was water worked at the highest discharge, and lower discharge flow field measurements took place subsequently. Cooper et al. (2013) used the same dataset as obtained by Aberle et al. (2008), as well data from Cooper and Tait (2010) and showed that form-induced stress was more significant at smaller flow depths.

Although those recent studies substantially improved our understanding of near-bed flow fields, there is a need to alleviate some of the challenges researchers of mobile boundary near-bed flow fields face. One way to simplify the system boundaries is to use fixed beds, thus allowing repeatable flow measurements, as well as studying the effect of submergence and discharge on the same topography. In the past, Buffin-Bélanger et al. (2003) used a casting technique to successfully mold natural river-bed surfaces with millimetre scale errors (0.5 per cent of the microrelief). More recently, Rice et al. (2014) used the same casting technique to obtain three molds of different water-worked gravel beds. Rice et al. (2014) did show that the integral flow characteristics

in the roughness layer vary for different gravel-bed microtopographies.

Spiller et al. (2012) improved Buffin-Bellanger's molding technique by using silicone rubber instead of Polyvinyl chloride (Gelflex™). The silicone-rubber does not have to be heated and will not be destroyed during the casting process, so that it can be used to produce several streambed duplicates. In addition, Spiller et al.'s (2012) technique does not require a rigid component of the mold, such as polyurethane foam resin, which Buffin-Belanger stated to be "essential".

Based on the work Rice et al. (2014) did, using acoustic Doppler velocimeter measurements of the interfacial layer, the objective of the present study is to obtain high spatial resolution 3D near-bed flow fields by employing a Vectrino II acoustic Doppler velocimeter. Rice et al. (2014) obtained flow data for 99 nodes, aligned on a rectangular grid of 0.8-m length and 0.5-m width, with 9 measurements spaced regularly (every 100-mm) in flow direction, and 11 measurements spaced regularly (every 50-mm) across the flow. For this study, detailed measurements are obtained for a region of interest constituting 425 nodes, aligned on a dense rectangular grid of 0.150-m length and 0.102-m width, with a regular spacing of 6-mm between grid nodes. Data is obtained for the full extent of a Vectrino II profiler – 34-mm.

1.1 *Bed roughness*

A challenge for all bed roughness studies is the determination and definition of roughness heights. For gravel beds, made up of relatively uniformly distributed particles, the roughness height is similar to the diameter of the particle. Raupach et al. (1991) first introduced a roughness region, with a thickness of two to five times the roughness height. More recently, Nikora et al. (2001) introduced the definition of a roughness layer, made up of the interfacial sublayer and the form-induced sublayer. As pointed out by Nikora et al. (2001), the definition of a reference bed, and the thickness of the interfacial sublayer are challenging. The correct definition of the reference bed is important for collected flow data to be aligning with known logarithmic flow profiles, as summarised by Smart (1999). Aberle et al. (2008) showed that hydraulic data can be used to define the roughness crest for rough, irregular beds, but they were not able to define the extent of the roughness layer from the obtained hydraulic data. For the present study, the figures are shown in relation to the flow measurements extension. As the objective of the paper is the presentation of near-bed flow fields, without detailed qualitative analysis of their relations to the roughness region, this approach is deemed acceptable.

2 METHODOLOGY

2.1 *Experimental setup*

The experiments were undertaken at the Fluid Mechanics Laboratory of the University of Auckland. The flume in use is 19-m long, 0.45-m wide and 0.5-m deep. The flume slope for this study is fixed and set to 0.005. A mold of an armoured gravel bed (Spiller et al. 2012) is fixed to the flume floor. The mold is 0.2-m wide, and placed in the centre of the flume. Due to the mold not covering the whole width of the flume, the sides are covered with mold offcuts from a second mold, thus ensuring roughness uniformity, with the remaining gap at the flume side walls covered with smooth PVC bars. To ensure roughness adjustment, the test section upstream end is covered with roughness elements of similar geometry. The fixed gravel bed has the following properties: d_{50}=13.5-mm, d_{84}=23-mm (Spiller et al. 2012). The study is undertaken in uniform and steady flow conditions. The paper presents results from one discharge, 49.2-l/s, with a water depth of 140-mm above the roughness crests. The discharge was set by opening a valve at the beginning of an experiment, and was not changed until the measurements were finished for the specific flow rate.

2.2 *DEM*

Although using molds does simplify the system boundaries for near-bed flow studies, one remaining challenge is the direct spatial correlation of measured flow characteristics to a known system boundary. Recently, the research group at the University of Auckland developed an advanced stereo vision system to measure underwater topographies in a laboratory environment. Its usability is compared with other bed-roughness measurement techniques and evaluated in Bertin and Friedrich (2014). Using a 3D printed model did allow the evaluation of the feature matching (Bertin et al. 2014), ensuring reliable Digital Elevation Model (DEM) generation, resolving at over 30million points/m^2. Using the procedure as presented in Bertin et al. (2013), a DEM of the gravel-bed mold (Spiller et al. 2012) was obtained (Figure 1), using a uniform sampling distance of 0.25-mm.

2.3 *Flow measurement*

Acoustic Doppler velocimeters are widely available over the last 20 years. García et al. (2005); Lohrmann et al. (1994); McLelland and Nicholas (2000) provide detailed technical and operational information on the use of the acoustic Doppler velocimeters. Nortek's Vectrino II Profiler was released in

2011, and measures up to 34 three-component velocity data series', with a fourth redundant velocity, along a profile. It has a central sound transmitter and 4 sound receivers. The closest profile location sampled is 40-mm away from the central transmitter, with the furthest profile location sampled 74-mm away from the central transmitter.

Nortek's Vectrino II Profiler does not require user calibration. It is factory calibrated, by determining the probe head geometry with tow tank calibration. For the present study, user input settings were determined during preliminary testing.

Acoustic Doppler velocimeter measurements use Taylor's hypothesis to obtain flow data records. It is assumed that the turbulence characteristics are frozen within the sampling volume, with the characteristic size being the larger of the sampling diameter and the sampling height. For the present study, the sampling diameter of 6-mm, which is a constant variable for the Vectrino II, is the characteristic size used to measure the size of turbulent eddies, which can be analysed for a certain mean flow.

The Vectrino II Profiler, similarly to the Vectrino single-point velocimeters, has three general error sources, namely (1) sampling hardware errors, (2) Doppler noise and (3) high shear in the sampling volume (McLelland and Nicholas 2000). Commonly, average velocities and Reynolds stresses are obtained with acoustic Doppler velocimeters, as the inherent Doppler noise is unbiased for the average velocities, and assuming an even noise level for all recording channels, the instantaneous fluctuations can be used for accurate Reynolds stress estimation (Lohrmann et al. 1995).

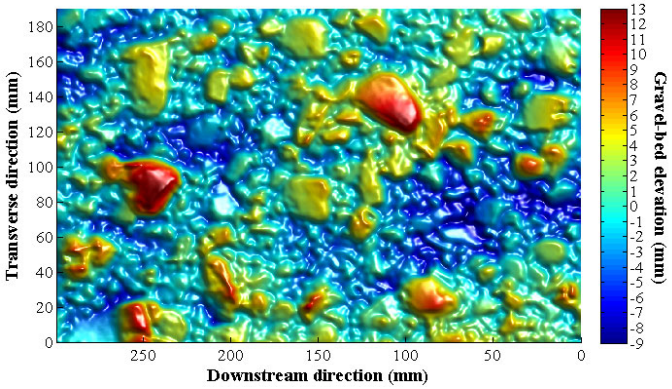

Figure 1. DEM of gravel-bed mold.

2.4 *Region of interest*

Due to the Vectrino II's sampling diameter of 6-mm, the node distance was set at 6-mm in both, streamwise and across flow directions. A uniform, rectangular measurement area was chosen, with 25 measurements spaced regularly in flow direction, and 17 measurements spaced regularly across the flow, resulting in 425 measurement locations all together, covering a dense rectangular grid of 0.150-m length and 0.102-m width. For the following figures, the coordinate origin is set in the centre of the region of interest, as shown in Figure 2. A uniform sampling distance of 0.25-mm results in 601 x 409 DEM data points for the region of interest.

2.5 *Flow analysis*

All 425 flow data series' were recorded at a sampling rate of 100Hz, for 120-sec. During the recording, which extended beyond one day, the flow was not turned off, to ensure constant discharge. After data recording, a MATLAB routine was used to read all data files, undertake the pre-processing to correct for communication errors and despiking (Goring and Nikora 2002). Figure 3 shows the percentage of good data after pre-processing for slice 9.

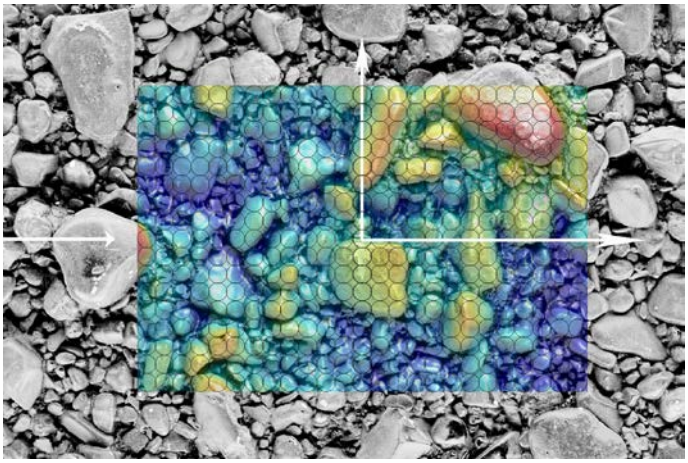

Figure 2. Region of interest, with DEM overlaid, and identification of all 425 individual measurement locations. Flow direction is indicated with left arrow. Each row of measurement locations in this Figure represents a vertical slice of the flow field (as used for Figures 3-5) and is numbered from bottom (slice 1) to top (slice 17).

3 RESULTS AND DISCUSSIONS

This paper concentrates on the preliminary presentation of average flow velocities. For all following figures, the flow is from left to right.

3.1 *Slices of vertical flow fields in flow direction*

To align known boundary information to suit the flow field measurements, the DEM samples need to be related to the flow sample volume. If the acoustic Doppler velocimeter's sample volume comes in touch with the gravel-bed boundary, the data for that part of the profile will be contaminated. No information is available on what is the closest distance away from a boundary for which acoustic Doppler velocimeter techniques provides accurate data. Dey et al. (2012), for their study of turbulence in mobile streams, made sure the closest boundary measure-

ments are 2-mm away from the mobile surface. For the present paper, due to the 6-mm sampling diameter for the flow field studies, each flow measurement node occupies 25 DEM data points, at the used sampling distance of 0.25-mm, with neighboring nodes sharing the same data point at the perimeter. To ensure the sampling volume does not interfere with the gravel bed, the maximum value of a group of 25 DEM data points across the width of a slice is used to assign the gravel boundary, as shown in Figures 3-5.

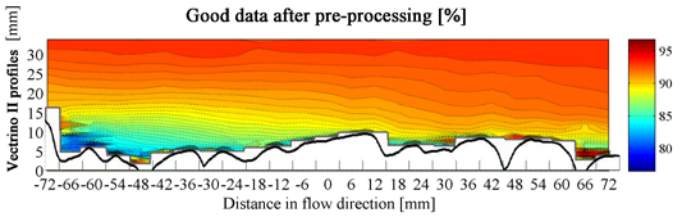

Figure 3. Percentage of good data after pre-processing for slice 9. Shown is the DEM profile (maximum value across the slice width) for all DEM data points in flow direction (black line), as well as the maximum for the squared surface area (25 x 25 data points), which occupies the 6-mm acoustic Doppler velocimeter sample volume, for each of the 25 sampling locations in flow direction (grey line).

Figure 3 shows both, the maximum DEM data point across the width of a slice (black line), for each data point along the region of interest, as well as the maximum elevation for the area corresponding to the 6-mm sampling node (grey line). The grey line thus represents the maximum penetration of the gravel-bed visible for each of the acoustic Doppler velocimeter samples. The velocimeter probe was aligned manually with the help of a ruler, and care was taken to adjust both the horizontal as well as the vertical positioning as accurately as possible. As can be seen in Figure 3, some measurement nodes close to the boundary exhibit random noise. It is also shown that data quality reduces in locations strongly influenced by roughness elements, and thus locations of more pronounced decelerations and accelerations, such as behind the major roughness element at the upstream end of the slice in Figure 3.

Figures 4 and 5 represent average flow information for selected vertical slices. Figure 4 shows all three spatial mean velocities for slice 1, whereas Figure 5 shows the distribution of the mean streamwise velocity for all slices.

As can be seen from Figure 4, there is a major roughness element (at -50-mm distance along the flow), which affects velocity components in all three spatial scales, not only in the interfacial layer, but also above the roughness tops visible for that slice. For the streamwise velocity component, a separation zone extends to the next major downstream roughness element (at 40-mm distance along the flow). From Figure 2 one can see that slice 1 as at the outer area of flow measurements undertaken. The dominating upstream roughness element of this slice is deposited across the flow, which explains the visible strong separation for over half the streamwise length of this specific region of interest. The approaching flow for that major roughness element is characterised by a deceleration in the streamwise component, together with strong acceleration in the vertical flow component. The separation zone downstream of the roughness element shows a negative vertical velocity component, as well as a negative across flow component, indicating that the across flow comes from the true left side of the flume. Figure 2 can be used again to better understand the nature of the across flow. As the roughness element extends further to the true right side of the flow, the observed negative across flow pattern results from the flow around the gravel particle's true left side.

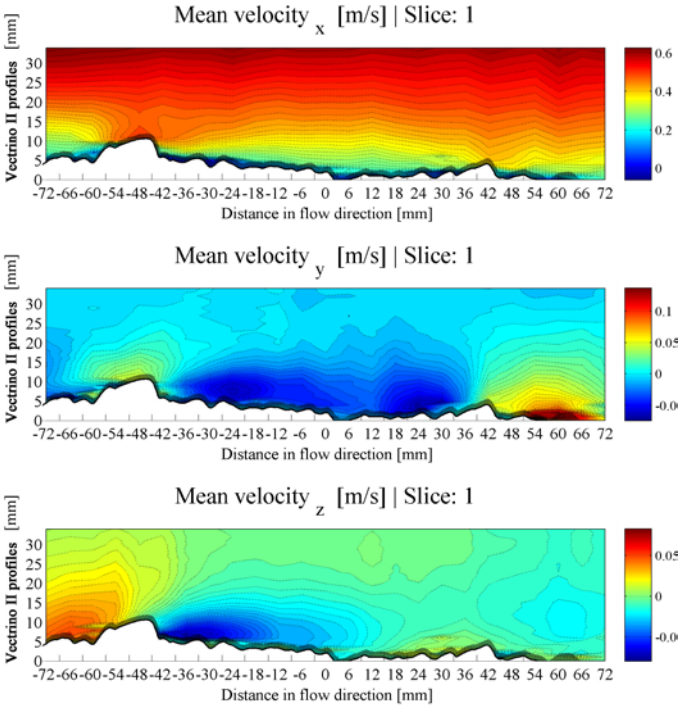

Figure 4. Average decomposed flow information for all three spatial direction for vertical slice 1.

Figure 5 shows streamwise velocity components for all 17 slices, with the centreline slice (9) at top. One can clearly see how the roughness elements affect the flow, with only the measurement nodes at the highest elevations displaying roughness-unaffected streamwise velocity components. The streamwise velocity component in slice 6 for instant, although not displaying a major roughness element as some of the other slices, is profoundly influenced by the roughness element just upstream of the region of interest (Figure 2), with the wake visible in most of slice 6.

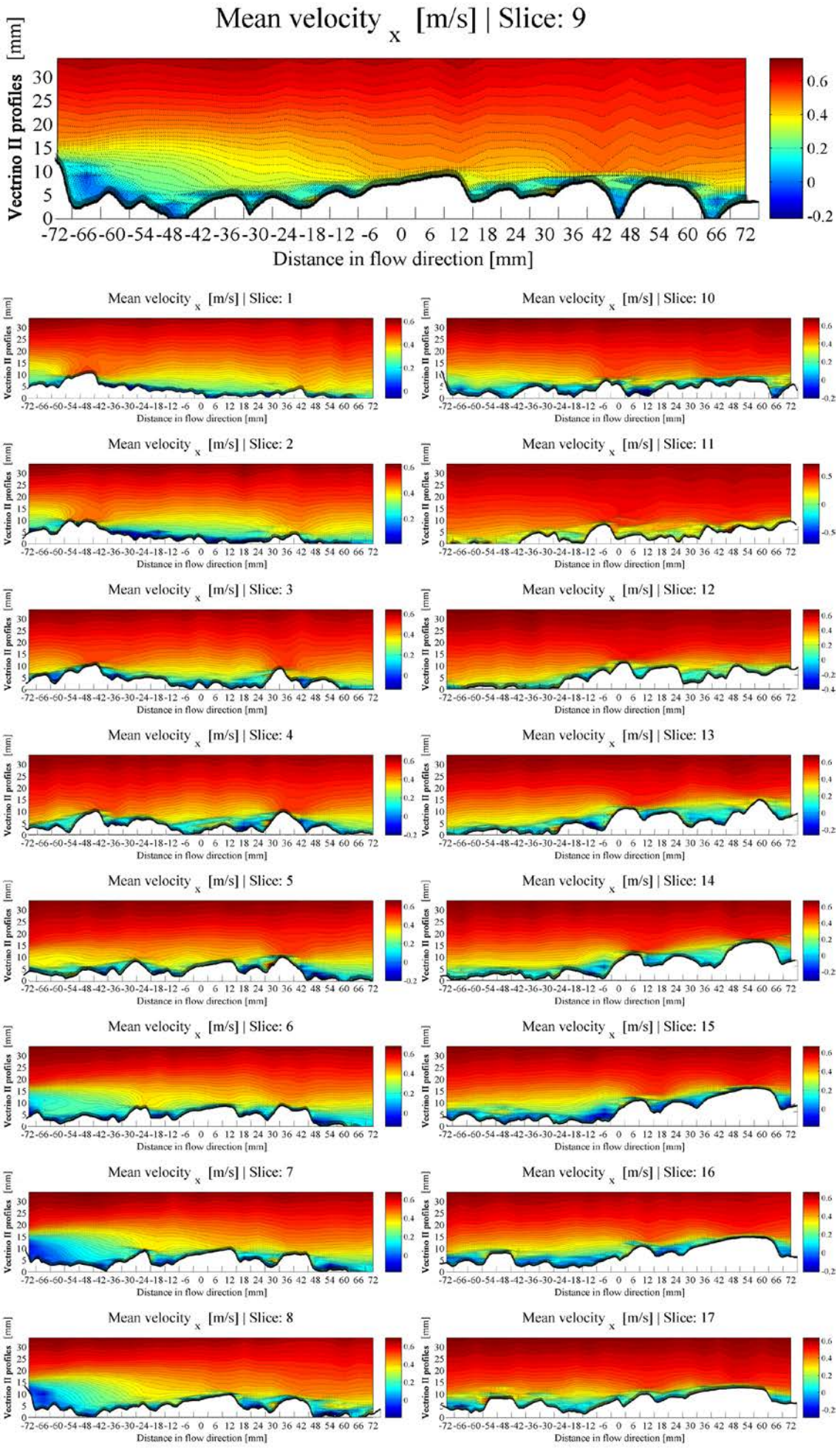

Figure 5. Average streamwise flow information for all vertical slices.

3.2 *Layers of horizontal flow fields*

The obtained data also allow the display of horizontal flow field layers overlaid with the bed topography or DEM. A qualitative representation of the 2D flow field just above the highest roughness top in the region of interest is shown in Figure 6. One can clearly see how the previously referred to roughness element just upstream of the region of interest influences the 2D flow magnitude immediately downstream of its presence. For this layer just above the interfacial roughness zone there is a considerable slowed-down flow area visible. Similarly, the relative smooth area to the true left and just downstream of the coordinate origin acts as a funnel for higher than average flows. This funnel is initially caused by the area's upstream gap between the gravel particle in the middle of the region of interest and the gravel particle deposited across flow further to the true left. In addition, this accelerated flow path is strengthened by flow passing by the downstream major roughness element in the top right of the region of interest (Figure 6).

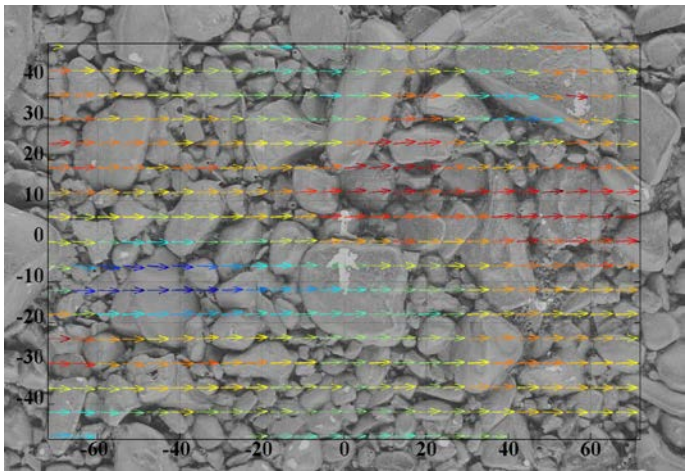

Figure 6. Qualitative representation of the 2D flow field (streamwise and across flow) just above the highest roughness top for the region of interest. Red = high flow magnitude, blue = low flow magnitude.

4 CONCLUSION

The paper presents initial results from a comprehensive project on near-bed gravel-bed flow fields. The experimental environment is presented, as well as the various techniques employed for this study, namely casting of a fixed-bed mold, stereo vision to obtain a DEM of the mold and Vectrino II profiler measurements to obtain 3D flow field information for an identified region of interest. The presented results concentrate on selected average flow distributions along the flow, as well as a horizontal flow field layer just above the roughness tops. The potential of the data to be used to better quantify the effect of roughness on the near-bed flow field is shown. The next step is to quantitatively relate flow information to the roughness reference bed. The data allows studying the extend roughness influences the flow field outside the interfacial layer. This will contribute to our present knowledge, such as that spatial flow variance is roughly five times higher within the roughness layer than above (Cooper et al. 2013) found. Only results from one discharge are presented herewith, thus the role of relative submergence needs to be addressed with a change of flow rate and water depth.

5 ACKNOWLEDGEMENTS

The authors would like to thank Stephane Bertin for obtaining the DEM used for the study. The experimental data was obtained as part of an undergraduate research project by students Ziwen An and Chenhui Zhou.

6 REFERENCES

Aberle, J., Koll, K., and Dittrich, A. (2008). "Form induced stresses over rough gravel-beds." *Acta Geophysica*, 56(3), 584-600.

Bertin, S., and Friedrich, H. (2014). "Measurement of gravel-Bed Topography: An Evaluation Study Applying Statistical Roughness Analysis." *Journal of Hydraulic Engineering*, 140(3), 269–279.

Bertin, S., Friedrich, H., Delmas, P., and Chan, E. (2013). "The Use of Close-Range Digital Stereo-Photogrammetry to Measure Gravel-Bed Topography in a Laboratory Environment." *Proc. 35th IAHR Congress*, Chengdu, China, September 8-13, 12pp.

Bertin, S., Friedrich, H., Delmas, P., Chan, E., and Gimel'farb, G. (2014). "DEM quality assessment with a 3D printed gravel bed in application to stereo photogrammetry." *submitted to Photogrammetric Record*.

Buffin-Bélanger, T., Reid, I., Rice, S., Chandler, J. H., and Lancaster, J. (2003). "A casting procedure for reproducing coarse-grained sedimentary surfaces." *Earth Surface Processes and Landforms*, 28(7), 787-796.

Cooper, J. R., Aberle, J., Koll, K., and Tait, S. J. (2013). "Influence of relative submergence on spatial variance and form-induced stress of gravel-bed flows." *Water Resources Research*, 49(9), 5765-5777.

Cooper, J. R., and Tait, S. J. (2010). "Spatially representative velocity measurement over water-worked gravel beds." *Water Resources Research*, 46(11).

Dey, S., Das, R., Gaudio, R., and Bose, S. K. (2012). "Turbulence in mobile-bed streams." *Acta Geophysica*, 60(6), 1547-1588.

García, C. M., Cantero, M. I., Niño, Y., and García, M. H. (2005). "Turbulence measurements

with acoustic doppler velocimeters." *Journal of Hydraulic Engineering*, 131(12), 1062-1073.

Goring, D. G., and Nikora, V. I. (2002). "Despiking acoustic doppler velocimeter data." *Journal of Hydraulic Engineering*, 128(1), 117-126.

Lohrmann, A., Cabrera, R., Gelfenbaum, G., and Haines, J. (1995). "Direct measurements of Reynolds stress with an acoustic Doppler velocimeter." *Proceedings of the 1995 5th IEEE Working Conference on Current Measurement*, 205-210.

Lohrmann, A., Cabrera, R., and Kraus, N. C. (1994). "Acoustic-doppler velocimeter (ADV) for laboratory use." *Proceedings of the Symposium on Fundamentals and Advancements in Hydraulic Measurements and Experimentation*, 351-365.

McLelland, S. J., and Nicholas, A. P. (2000). "A new method for evaluating errors in high-frequency ADV measurements." *Hydrological Processes*, 14(2), 351-366.

Nikora, V., Goring, D., McEwan, I., and Griffith, G. (2001). "Spatially averaged open-channel flow over rough bed." *Journal of Hydraulic Engineering*, 127(2), 123-133.

Raupach, M. R., Antonia, R. A., and Rajagopalan, S. (1991). "Rough-wall turbulent boundary layers." *Appl. Mech. Rev.*, 44(1), 1-25.

Rice, S. P., Buffin-Bélanger, T., and Reid, I. (2014). "Sensitivity of interfacial hydraulics to the microtopographic roughness of water-lain gravels." *Earth Surface Processes and Landforms*, 39(2), 184-199.

Smart, G. M. (1999). "Turbulent velocity profiles and boundary shear in gravel bed rivers." *Journal of Hydraulic Engineering*, 125(2), 106-116.

Spiller, S., Rüther, N., and Baumann, B. (2012). "Artificial reproduction of the surface structure in a gravel bed." *2nd IAHR Europe Congress*, München, Germany.